8196–8209 *Nucleic Acids Research, 2013, Vol. 41, No. 17* *Published online 4 July 2013*
doi:10.1093/nar/gkt564

Involvement of *Schizosaccharomyces pombe rrp1*$^{+}$ and *rrp2*$^{+}$ in the Srs2- and Swi5/Sfr1-dependent pathway in response to DNA damage and replication inhibition

Dorota Dziadkowiec[1,*], Karol Kramarz[1], Karolina Kanik[1], Piotr Wiśniewski[2] and Antony M. Carr[3]

[1]Faculty of Biotechnology, Wrocław University, Przybyszewskiego 63-77, 51-148 Wrocław, Poland, [2]Institute of Low Temperature and Structure Research, Polish Academy of Sciences, PO Box 1410, 50-950 Wrocław, Poland and [3]Genome Damage and Stability Centre, University of Sussex, Falmer, Brighton, BN1 9RQ, UK

Received April 15, 2013; Revised June 1, 2013; Accepted June 4, 2013

ABSTRACT

Previously we identified Rrp1 and Rrp2 as two proteins required for the Sfr1/Swi5-dependent branch of homologous recombination (HR) in *Schizosaccharomyces pombe*. Here we use a yeast two-hybrid approach to demonstrate that Rrp1 and Rrp2 can interact with each other and with Swi5, an HR mediator protein. Rrp1 and Rrp2 form co-localizing methyl methanesulphonate–induced foci in nuclei, further suggesting they function as a complex. To place the Rrp1/2 proteins more accurately within HR sub-pathways, we carried out extensive epistasis analysis between mutants defining Rrp1/2, Rad51 (recombinase), Swi5 and Rad57 (HR-mediators) plus the anti-recombinogenic helicases Srs2 and Rqh1. We confirm that Rrp1 and Rrp2 act together with Srs2 and Swi5 and independently of Rad57 and show that Rqh1 also acts independently of Rrp1/2. Mutants devoid of Srs2 are characterized by elevated recombination frequency with a concomitant increase in the percentage of conversion-type recombinants. Strains devoid of Rrp1 or Rrp2 did not show a change in HR frequency, but the number of conversion-type recombinants was increased, suggesting a possible function for Rrp1/2 with Srs2 in counteracting Rad51 activity. Our data allow us to propose a model placing Rrp1 and Rrp2 functioning together with Swi5 and Srs2 in a synthesis-dependent strand annealing HR repair pathway.

INTRODUCTION

In all organisms, homologous recombination (HR) is a high-fidelity DNA repair pathway, essential for the repair of DNA double-strand breaks (DSBs) and for normal DNA replication. The RecA/Rad51 family of proteins forms filaments on single-stranded DNA (ssDNA), which catalyze homology search DNA strand invasion reactions, the hallmark of HR (1). Nucleofilament formation by Rad51 recombinase (formerly Rhp51 in *Schizosaccharomyces pombe*) (2) is assisted by a group of proteins called recombination mediators (3–5). The main mediator, Rad52 (formerly Rad22 in *S. pombe*), localizes to the 3′ ends of ssDNA and is required for the exchange of RPA for Rad51 (6–8). Human and mice homologs of Rad52 exist but are thought to play a minor role in vertebrate HR; for example, knockout mice exhibit almost no phenotype in DNA recombination or repair (9). In its place, the human tumor suppressor protein BRCA2 plays a key role in HR, recruiting vertebrate RAD51 on RPA-coated ssDNA and stabilizing presynaptic filaments (10,11). Recently, vertebrate RAD52 has been shown, especially in the absence of BRCA2, to anneal RPA-coated ssDNA (12,13).

Additional proteins or complexes are required to facilitate the formation and/or stabilization of the Rad51 nucleoprotein filament. The Rad55/Rad57 complex (formerly Rhp55/Rhp57 in *S. pombe*) was shown to stabilize the Rad51 nucleofilament and enhance Rad51-mediated strand exchange (14–16). In *Saccharomyces cerevisiae*, the Rad55/Rad57 heterodimer counteracts the disruption of nucleoprotein filament by the Srs2 antirecombinase in a manner requiring direct interaction between Rad55/Rad57 and Srs2 (17). In *S. pombe*, a

*To whom correspondence should be addressed. Tel: +4871 375 6238; Fax: +4871 375 6234; Email: dorota.dziadkowiec@uni.wroc.pl
Present address:
Karol Kramarz, Faculty of Biological Sciences, University of Wrocław, 51-148 Wrocław, Poland.

second mediator complex, Sfr1/Swi5 (18) acts in parallel to Rad55/Rad57 (19,20) to stabilize and activate Rad51-ssDNA filaments in an ATP-dependent manner (21). Sfr1/Swi5 is conserved in mice and humans, and its depletion results in sensitivity to ionizing radiation, suggesting a conserved role in HR (22,23). A corresponding complex in *S. cerevisiae*, Sae3/Mei5 functions exclusively in meiosis together with Dmc1, the meiotic Rad51 homolog (24,25).

HR plays a critical role in both DSB DNA repair and in the recovery of arrested replication forks (26–28). In the absence of HR, spontaneously occurring barriers to replication fork progression contribute to a slow growth phenotype and to constitutive checkpoint activation. ssDNA is a common intermediate in many aspects of DNA metabolism including replication arrest and can promote inappropriate recombination that, in turn, leads to genomic instability (29). Thus, the action of Rad51 and its mediators must be tightly controlled. There is substantial evidence that the choice of a mediator complex may determine the final outcomes of HR: for example, Rad55/Rad57, but not Swi5/Sfr1, is essential for crossover (CO) production in *S. pombe* (30,31). Selection of the mechanism for recombination intermediate resolution is also important: for example, the Mus81-Eme1 nuclease complex is required for CO formation in mitotic cells (32).

On the other hand, the role of numerous noncanonical helicases in recombination is to restrict the formation of CO. Anti-recombinogenic helicases Srs2 and Fml1 (FANCM ortholog) are essential for CO avoidance, acting to remove Rad51 from ssDNA and channel repair into synthesis-dependent strand annealing (SDSA) (33–37). The RecQ homologs act as anti-recombinases by promoting Holiday junction (HJ) dissolution thus limiting CO formation (33,38). In *S. pombe*, an F-box helicase, Fbh1, has also been shown to limit CO formation, particularly at stalled replication forks (39–41). Inappropriate activation of HR can lead to erroneous recombination, promoting genetic instability, loss of heterozygosity, chromosome rearrangements and potentially cell death. Thus, identifying all the players and understanding of the interactions between Rad51 recombinase, its mediators plus the enzymes that can remodel and/or resolve joint molecules is crucial for building a model of HR regulation in mitotic cells. *Schizosaccharomyces pombe* has proven a good model system for this purpose: two new mediator complexes, Swi5/Sfr1 (18) and Rrp1/Rrp2 (42), were initially identified in this organism. Here we present further characterization of the Rrp1 and Rrp2 proteins. We show that they can form a complex with each other and co-localize at sites of DNA damage. We present genetic evidence that Rrp1 and Rrp2 act together in a Srs2- and Swi5/Sfr1-dependent SDSA sub-pathway of HR for DSB repair and replication-dependent DNA damage tolerance.

MATERIALS AND METHODS

Strains and plasmids

Strains used in this work (Supplementary Table S1) are derived from the parental strain YA 254.

Media and general methods

Media used for *S. pombe* growth were as described (43). Yeast cells were cultured at 30°C in complete yeast extract plus supplements (YES) medium or Edinburgh minimal medium (EMM). Thiamine was added, where required, at 5 μg/ml and geneticin (ICN Biomedicals) at 100 μg/ml. For YES low Ade plates, the concentration of adenine was reduced 10-fold.

Spot assays

Cells were grown to mid log phase, serially 10-fold diluted and 2 μl aliquots were spotted onto YES plates, which were either UV irradiated using Stratalinker (Stratagene) or contained one of the following compounds: methyl methanesulphonate (MMS), camptothecin (CPT) or hydroxyurea (HU) at the stated concentrations. Plates were incubated at 30°C for 3–5 days and photographed. All assays were repeated a minimum of three times.

Complementation of *rad57Δrrp2Δ* mutant phenotype by overexpression of Rrp2

The *rrp2*$^{+}$ gene was polymerase chain reaction amplified using genomic DNA as a template and cloned into the *NdeI-SmaI* sites of pREP41/42-EGFPN (44), or into *SalI-SmaI* sites of pREP41-Red Fluorescent Protein (RFP) plasmid (42). Both inserts were verified by sequencing. For complementation experiments, *rad57Δ rrp2Δ* mutant cells transformed with either pREP41-RFP-Rrp2 or the empty vector control were grown for 20 h in EMM-Leu medium without thiamine. Both cultures were diluted and 2 μl aliquots were spotted on YES plates either without drug or containing 1.5 μM CPT or 4 mM HU. Untransformed *rad57Δ* and *rad57Δ rrp2Δ* mutant cultures were plated for comparison.

Survival assays

For CPT survival, cells were grown to mid-log phase in 5 ml YES medium, CPT was added to a final concentration of 20 μM and cultures incubated at 30°C. At the stated timepoints, 500 μl aliquots were removed to Eppendorf tubes, serially diluted and plated on YES plates. Plates were incubated at 30°C for 3–5 days. Colonies formed were counted and percent survival calculated against samples taken before addition of the drug (time 0).

For HU survival, cells were grown to mid-log phase in 5 ml YES medium, serially diluted and plated on YES plates containing the indicated concentrations of HU. Colonies formed after 4–6 days of incubation were counted and percent survival calculated against the no drug control. All assays were repeated a minimum of three times for each strain.

For survival following acute HU treatment, cells were grown to mid-log phase in 5 ml YES medium and samples were taken, serially diluted and plated on YES medium to determine the initial number of cells in each culture. To the remaining culture, HU was added to a final concentration of 12 mM. Cells were incubated at 30°C for 4 h, washed, resuspended in 5 ml of fresh YES medium and allowed 4 h recovery at 30°C. Samples were taken for

fluorescence microscopy examination (processed as described below), while the remaining culture was serially diluted and plated on YES medium to determine the number of viable cells in each culture following recovery from acute HU treatment.

Fluorescence microscopy

Samples taken after recovery from acute HU treatments were washed and fixed in 70% ethanol. After rehydration, cells were stained with 1 μg/ml 4',6-diamidino-2-phenylindole (DAPI) and 1 mg/ml *p*-phenylenediamine in 50% glycerol and examined by fluorescence microscopy. To determine the cellular localization of Rrp1 and Rrp2 proteins in strains devoid of the Rad51 recombinase or the Rad57 and Swi5 mediator proteins, respective mutants were transformed with pREP42-EGFP-Rrp1 or pREP42-EGFP-Rrp2, grown for 20 h in EMM medium without uracil or thiamine (to induce the expression of respective proteins) and subsequently divided into two parts. One part was incubated for 1 h in 0.1% MMS, the other served as untreated control. Cells were subsequently washed with 20% $Na_2S_2O_3$ to inactivate MMS, washed with water and observed by fluorescence microscopy using an Axio Lab.A1 microscope (Carl Zeiss). Images were captured using a Canon digital camera and processed with Axiovision 4.8.

Co-localization experiments

KAF1448 (Rad52-GFP::KANMX6) was transformed with pREP41-RFP-Rrp2 and transformants were selected on EMM-Leu plates containing thiamine (5 μg/ml). RFP-Rrp2 expression was induced by 20 h incubation in EMM-Leu without thiamine. Cells were subsequently treated with 0.1% MMS for 1 h, washed in 20% $Na_2S_2O_3$, washed with water and visualized by fluorescence microscopy. To determine the co-localization of Rrp1 and Rrp2, a wild-type strain was cotransformed with pREP42-EGFP-Rrp1 and pREP41-RFP-Rrp2 and transformants were selected on EMM-Leu-Ura plates containing thiamine (5 μg/ml). After induction of both proteins by 20 h growth in EMM-Leu-Ura without thiamine, cells were treated with 0.1% MMS as described above and visualized by fluorescence microscopy.

Yeast two-hybrid assay

Gal4-based Matchmaker Two-Hybrid System 3 (Clontech) was used for the yeast two-hybrid assay according to manufacturer's instructions. The indicated proteins were fused to the GAL4 activation domain (AD) in pGADT7 vector and the GAL4 DNA-binding domain (DBD) in pGBKT7, and expressed in *S. cerevisiae* tester strain AH109. Transformants were selected on synthetic dextrose drop-out medium without Leu and Trp (SD DO-2), and then plated on medium and high stringency drop-out media without Leu, Trp and His (SD DO-3) and without Leu, Trp, His and Ade (SD DO-4), respectively. Self-activation observed when the studied protein is fused to AD domain may indicate the ability of protein to bind DNA self-activation observed when the studied protein is fused to DBD domain likely suggests the protein's ability to induce transcription via the nonspecific recruitment of transcription factors.

Recombination assay

Spontaneous recombinant frequencies were measured as described (45). Single red (phenotypically *ade*$^-$) colonies representing the respective mutants were isolated from YES low-Ade plates, inoculated into liquid YES medium and grown to saturation. Appropriate dilutions were plated on YES plates to determine cell titre and on selective EMM-Ade plates to score the spontaneous Ade$^+$ recombinants. These were later replica plated on EMM-Ade-His plates to determine the proportion of conversion-type to deletion-type recombinants. At least five colonies from three independent experiments were examined for each strain and data are presented as a box and whiskers plot to highlight variation.

Detection of heavy molecular weight SUMO conjugates

Strains were grown in YES media at 30°C to late log phase (OD_{595} ~0.6), pelleted by centrifugation and total protein extracted by trichloroacetic acid (TCA) precipitation (46). The samples were resolved on a 4–16% gradient sodium dodecyl sulphate–polyacrylamide gel electrophoresis Biorad Gel and blotted onto Protran pure nitrocellulose membrane (Perkin Elmer). The membranes were stained for total protein with Ponceau S (Sigma-Aldrich) and then probed with anti-Pmt3 polyclonal serum (diluted 1:3000; a gift from Felicity Watts). Peroxidase-conjugated goat-anti-rabbit secondary antiobodies (diluted 1:5000, Sigma-Aldrich) were used to detect the primary antibody and these were revealed using an ECL detection kit (Perkin Elmer).

Pulse field gel electrophoresis

Cells were grown to mid-log phase in YES medium and samples from asynchronous (As) cultures taken for chromosome isolation. To the remaining cultures, HU was added to the final concentration of 16 mM and incubation continued for 4 h at 30°C. At that time, another set of samples was taken for chromosome isolation (HU) and the remaining cells were washed, resuspended in fresh YES medium and allowed to recover for 0.5, 1 and 2 h at 30°C at which timepoints samples were taken for chromosome isolation. Chromosomes were isolated using Biorad's CHEF Yeast Genomic DNA Plug Kit according to manufacturer's instructions with the following modifications: for each timepoint, 2×10^7 cells were harvested and embedded in 1% low melting point agarose in cell suspension buffer (10 mM Tris, pH 7.2, 20 mM NaCl, 100 mM EDTA) with 1 mg/ml lyticase. Plugs were allowed to solidify in 4°C and then digested for 2 h at 37°C in lyticase buffer (10 mM Tris, pH 7.2, 100 mM EDTA, 1 mg/ml lyticase). Next, plugs were washed with deionized water and transferred into a Proteinase K buffer (200 mM EDTA, pH 8.0, 0.2% sodium deoxycholate, 1% sodium lauryl sarcosine, 1 mg/ml Proteinase K) at 50°C. After 2 h, fresh Proteinase K buffer was added and plugs were incubated overnight at 50°C. The following day, after another buffer change, the

digestion was continued for 3 h at 50°C. Plugs were then washed four times (30 min each) in Tris-EDTA pH 8.0 and loaded into the wells of a 0.8% Multipurpose Agarose (Roche) gel. Gels were run on a Bio-Rad CHEF-DR-III pulse field gel electrophoresis (PFGE) system for 72 h at 14°C at 2.0 V/cm, angle 106°, 1800 s single switch time, pump speed 70. Separated chromosomes were stained in ethidium bromide (10 μg/ml) for 30 min, washed in deionized water for 3 h and visualized with UV transilluminator.

RESULTS

Rrp2 forms damage-associated foci in MMS-treated cells independently of Rad51, Rad57 and Swi5

We have previously shown (42) that both Rrp1 and Rrp2 function in the Swi5/Sfr1 sub-pathway of Rad51-dependent repair: *rad57*Δ *rrp1*Δ and *rad57*Δ *rrp2*Δ mutants are more sensitive to HU, CPT and MMS than the single *rad57*Δ mutant, and no such synergistic effect was observed for *sfr1*Δ *rrp1*Δ and *sfr1*Δ *rrp2*Δ mutants when compared with the single *sfr1*Δ mutant. We also demonstrated that Rrp1 co-localizes with MMS-induced Rad52 foci (42). To confirm our expectations that Rrp2 will show an equivalent localization to MMS-induced foci, we transformed a strain expressing Rad52-GFP (from the endogenous *rad52* promoter) with a plasmid carrying RFP-tagged Rrp2. As previously observed for Rrp1 (42), Rrp2 forms foci in the nucleus after 1 h of treatment with 0.1% MMS and 84% of these co-localized with Rad52-GFP (Figure 1a). We thus conclude that both Rrp1 and Rrp2 form foci in the nucleus that are associated with sites of DNA damage.

Using complementation analysis, we previously confirmed that the genetic interaction between *rrp1*Δ and *rad57*Δ was a direct result of the deletion of *rrp1*$^+$ (42). To confirm the analogous dependency on *rrp2*Δ for the increased sensitivity of the *rad57*Δ *rrp2*Δ mutant, we transformed the *rad57*Δ *rrp2*Δ cells with pREP41-RFP-Rrp2 or the empty vector control. Overexpression of RFP-Rrp2 complemented the CPT and HU sensitivity of *rad57*Δ *rrp2*Δ to the level of the single *rad57*Δ mutant (Figure 1b). These results support our earlier conclusion that both Rrp1 and Rrp2 participate in the HR DNA repair pathway and demonstrate that RFP-Rrp2 is functional.

Formation of Rad51 foci in response to UV is dependent on both Swi5 and Rad57, defining Rad55/57 and Sfr1/Swi5 as upstream of Rad51 foci formation (31). We sought to determine if MMS-induced Rrp1 and Rrp2 foci formation similarly relies on Swi5, Rad57 or Rad51. We transformed *rad51*Δ, *rad57*Δ and *swi5*Δ mutant cells with either pREP42-EGFP-Rrp1 or pREP42-EGFP-Rrp2 and examined the induced cultures after 1 h incubation in 0.1% MMS. Both Rrp1 and Rrp2 formed multiple foci in the nuclei of all three mutants (Figure 1c). We thus demonstrate that the Rrp1 and Rrp2 localize to the sites of DNA damage independently of Rad51, Rad57 or Swi5.

Rrp1 and Rrp2 can interact with each other and the Swi5 HR mediator protein

*rrp1*Δ and *rrp2*Δ share identical phenotypes, and the double *rrp1*Δ *rrp2*Δ mutant phenotype is no more severe compared with each single mutant. These data suggest that Rrp1 and Rrp2 could not substitute for each other's function and act nonredundantly (42). One explanation could be that Rrp1 and Rrp2 act in a common complex. To examine this possibility, we used the yeast two-hybrid system (Y2H) to examine potential interactions. We observed a strong interaction between Rrp1 and Rrp2, and a potential self-interaction for Rrp1, as judged by growth on high stringency SD DO-4 plates. Furthermore, both Rrp1 and Rrp2, when fused to the transcription activating domain, were capable of interacting with Swi5 (Figure 2a). Consistent with a potential interaction between Rrp1 and Rrp2, we further demonstrated that MMS treated cells that overexpress EGFP-Rrp1 and RFP-Rrp2 accumulate multiple foci in MMS treated cells in which EGFP and RFP signals co-localized in 87% of cases (Figure 2b). These results support conclusions from previous genetic analyses that Rrp1 and Rrp2 may work as a complex (42) and that this complex can localize to the sites of DNA damage.

Swi5-EGFP expressed from its own promoter forms weak spontaneous foci in the nucleus and the number of Swi5-EGFP foci was not significantly affected by MMS treatment (Supplementary Figure S1a). We were able to observe co-localization between genomically tagged Swi5-EGFP and overexpressed RFP-Rrp1 or RFP-Rrp2 in ~60% of cells (Supplementary Figure S1b). While these data are not conclusive, when taken together with the Y2H observation that suggests Rrp1 and Rrp2 are capable of interacting with Swi5, they may indicate a relationship between the Rrp1/Rrp2 interaction with the Swi5 mediator and aspects of Rrp1/Rrp2 function.

Rrp1 and Rrp2 can interact with SUMO but their loss does not lead to the increase in the heavy molecular weight SUMO conjugates

The primary Rrp1 and Rrp2 amino acid sequences share, respectively, 34 and 36% similarity to the C-terminal region of *S. cerevisiae* Uls1, a protein involved in replication stress response (42,47) that contains SNF2-N, RING finger and Helicase-C domains. Uls1 was identified as a two-hybrid interactor with yeast SUMO/Smt3 and contains four potential SUMO interacting motifs (SIM) in its N-terminus. In *S. cerevisiae*, *uls1*Δ mutant cells accumulated high molecular weight (HMW) SUMO conjugates. Uls1, together with Slx5-Slx8, human RNF4 and Rfp1-Slx8 and Rfp2-Slx8 from *S. pombe*, is thus a member of a class of proteins, the SUMO-targeted ubiquitin ligases (STUbLs), that are involved in targeting of SUMO-modified substrates for ubiquitin-mediated proteolysis (48,49).

Given the sequence similarity between Rrp1, Rrp2 and Uls1, we sought evidence that Rrp1 and Rrp2 might also belong to the STUbL family of proteins. Sequence analysis shows that Rrp1 contains a SIM consensus motif, (I/V)DL(T/D), which is also evident in *S. cerevisiae*

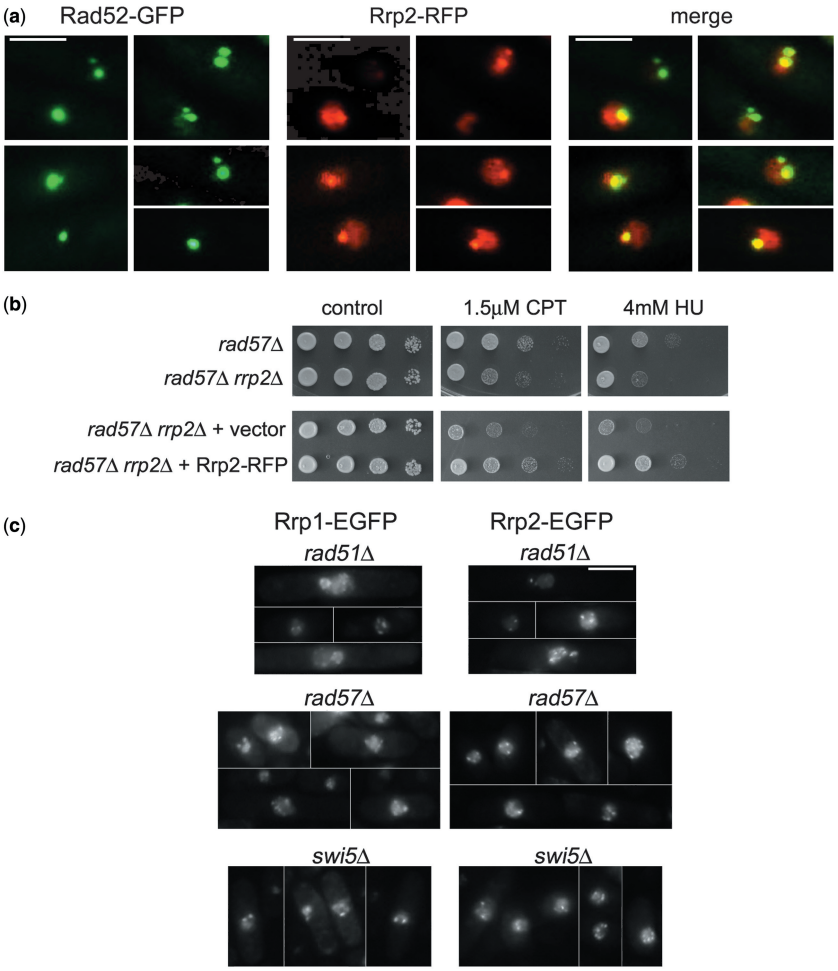

Figure 1. Involvement of Rrp1 and Rrp2 in HR. Co-localization of Rrp2-RFP foci with GFP-Rad22 nuclear foci formed on exposure to 0.1% MMS for 1 h (**a**). Complementation of the CPT and HU sensitivity of the *rad57*Δ *rrp2*Δ mutant by overexpression of Rrp2-RFP (**b**). Formation of Rrp1 and Rrp2 foci in the nucleus after MMS (1 h, 0.1%) treatment is not dependent on the presence of Rad51, Rad57 and Swi5 proteins (**c**). Scale bars = 10 μm.

Uls1, *S. pombe* Rfp1 and human RNF4 (Figure 2c) (48). A putative SIM was also identified in Rrp2, consisting of four hydrophobic residues surrounded by several acidic residues and potential phosphorylation sites. Similar motifs are found in Uls1 and RNF4 as well as in a potential SUMO-dependent isopeptidase from *S. cerevisiae*, Wss1 and the human SUMO-1–specific E3 ligase RanBP2 (Figure 2c) (48,50–52). Using Y2H analysis, we demonstrated that both Rrp1 and Rrp2 are able to interact with SUMO (Figure 2a).

We thus tested if *rrp1*Δ and *rrp2*Δ mutants accumulate HMW SUMO conjugates. The *rqh1*Δ mutant was examined as control because an *S. cerevisiae* strain devoid of the homologous Sgs1 protein accumulates HMW SUMO conjugates (53). Total protein extracts were prepared from logarithmic cultures and probed with anti-Pmt3 serum. No HMW bands were observed in a stacking gel for any of the tested strains. A small increase in the amount of HMW sumoylated proteins was apparent in the *rqh1*Δ extracts. However, neither of *rrp1*Δ, *rrp2*Δ and *rrp1*Δ *rrp2* Δ extracts displayed any evidence for increased HMW SUMO accumulation (Figure 2d). Thus, *rrp1*$^+$ and *rrp2*$^+$ do not significantly contribute to the global degradation of SUMO conjugated proteins in *S. pombe*.

Rrp1 and Rrp2 work with Srs2 within Swi5/Sfr1 sub-pathway of HR

We next examined the genetic interactions between *rrp1*$^+$ and *rrp2*$^+$ with the genes encoding two anti-recombinogenic helicases in *S. pombe*, *srs2*$^+$ and *rqh1*$^+$. Double *srs2*Δ *rrp1*Δ and *srs2*Δ *rrp2*Δ mutants have a phenotype equivalent to the *srs2*Δ single mutant when exposed to a range of genotoxic agents (Supplementary Figure S2a). The sensitivities observed for a double *rad51*Δ *srs2*Δ mutant was typical of that observed for *rad51*Δ· As expected, further deletion of *rrp1*$^+$ or *rrp2*$^+$ had no further effect (Figure 3a and Supplementary Figure S2b). This confirms that both Srs2 and Rrp1/Rrp2 work within the Rad51 pathway. As has previously been demonstrated for *srs2*Δ and *rad55*Δ (54), we observed a nonepistatic interaction between *srs2*Δ and *rad57*Δ on exposure to HU and CPT, suggesting that Srs2 and Rad57 may act in parallel independent sub-pathways within HR. Interestingly, concomitant deletion

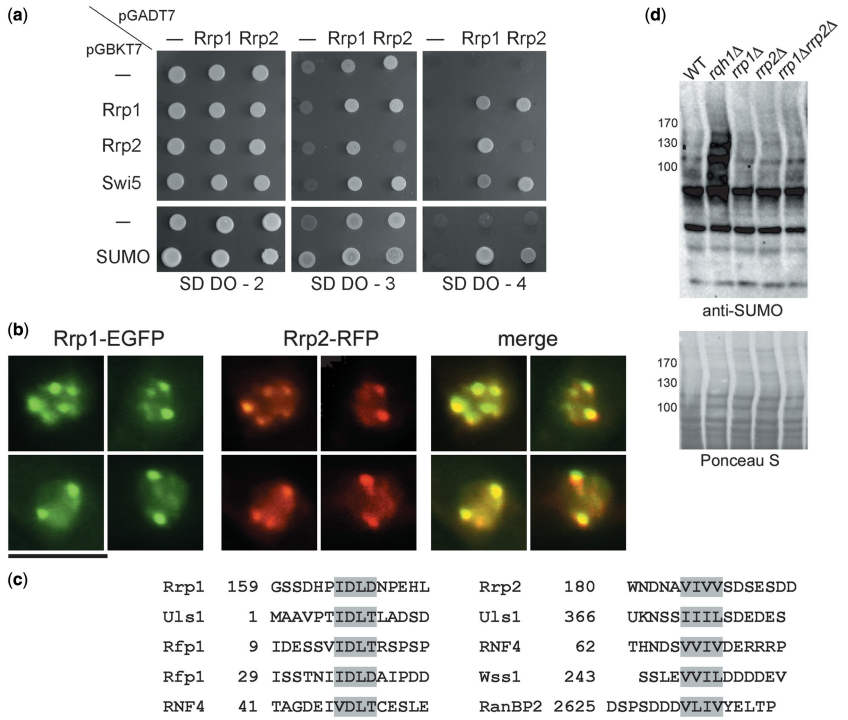

Figure 2. Interactions of Rrp1 and Rrp2 proteins. Rrp1 and Rrp2 can interact with each other, Swi5 and SUMO in the yeast two-hybrid system (**a**). Co-localization of Rrp1-EGFP and Rrp2-RFP nuclear foci after exposure to 0.1% MMS for 1 h (**b**). Scale bar represents 10 μm. Putative SUMO-interacting motifs found in the protein sequences of Rrp1 and Rrp2 (**c**). Analysis of the accumulation of heavy molecular weight SUMO conjugates in *rrp1*Δ and *rrp2*Δ mutants (**d**). Protein extracts were prepared from logarithmic cell cultures and probed with anti-Pmt3 serum (a gift from Felicity Watts).

of either $rrp1^+$ or $rrp2^+$ does not further increase the sensitivity (Figure 3a and b). Similar relationships were observed for MMS and UV (Supplementary Figure S2b). In our earlier work, we also demonstrated the existence of synergistic relationship of *rrp1*Δ and *rrp2*Δ with *rad57*Δ, which placed Rrp1 and Rrp2 function as parallel to the Rad55-Rad57 sub-pathway of HR (42). Taken together, these data suggest that Rrp1 and Rrp2 are functioning with Srs2, independently of Rad55-Rad57.

Given that Rad55-Rad57 is proposed to act in parallel to Swi5-Sfr1 in mediating Rad51-dependent recombination, we anticipated that *sfr1*Δ *srs2*Δ would be epistatic in our analysis. However, we observed a strong nonepistatic interaction between *srs2*Δ and both *swi5*Δ and *sfr1*Δ on CPT exposure, although this was not evident on HU, MMS or UV treatment. Again, the concomitant deletion of either $rrp1^+$ or $rrp2^+$ had no further effect (Figure 3c and d, and Supplementary Figure S2c). These data can be interpreted to place Rrp1/Rrp2 with Swi5/Sfr1 outside an Srs2-dependent pathway, at least for the repair of CPT-induced damage. These seemingly contradictory results can be reconciled within a model (Figure 4) based on that proposed by Akamatsu *et al.* (31). In this model, D-loop formation by Rad51 can be initiated by either the Rad55/Rad57 mediator function or by the Swi5/Sfr1 mediator. However, only the Rad55/Rad57 complex, but not Swi5/Sfr1 complex, can function during second end capture. Thus, the channeling of recombination into the canonical Szostack double HJ–dependent mode of double-strand break repair (DSBR) is proposed to be always Rad55/Rad57-dependent, irrespective of whether initial D-loop formation occurred via Rad55/Rad57 or via Swi5/Sfr1 mediator pathways. Conversely, the SDSA pathway can occur independently of Rad55/Rad57—D-loop formation initiated by Swi5/Sfr1—or via the mediator action of Rad55-Rad57 but without subsequent second-end capture.

In this scenario, Rrp1 and Rrp2 could work with Srs2 specifically within the SDSA branch of the Swi5/Sfr1-initiated sub-pathway of HR and be independent of Rad57. This would explain the epistatic nature of *rrp1*Δ/*rrp2*Δ mutants with *srs2*Δ. The observed nonepistatic CPT sensitivity observed between *swi5*Δ and *srs2*Δ in the *swi5*Δ *srs2*Δ double mutant would stem from the role of Srs2 in the Rad55/Rad57-initiated SDSA subpathway of HR, which we propose is independent of Rrp1 and Rrp2.

Antirecombinogenic activity of Rrp1 and Rrp2

While an ability to perform recombination is often reflected by an increased resistance to DNA-damaging agents, more subtle alterations in HR are characterized by changes in both the frequency at which spontaneous HR occurs and by the ratio between the potential outcomes of recombination. A common way to assay these in *S. pombe* is the HR-dependent restoration of gene activity between a tandem repeat containing two distinct *ade6* mutations that restore a functional allele by either gene conversion or HR-dependent gene deletion

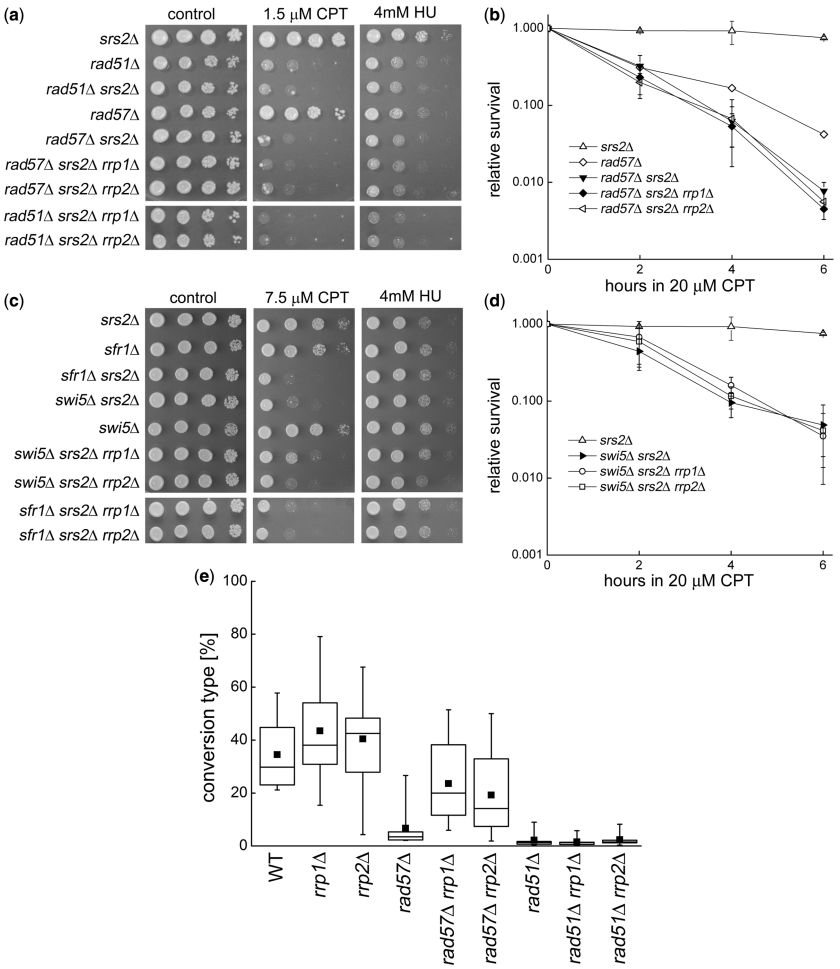

Figure 3. Epistasis between *rrp1*$^+$ and *rrp2*$^+$ and *srs2*$^+$ helicase gene. Comparison of the sensitivity to CPT and HU of *rrp1*Δ and *rrp2*Δ mutants in *rad51*Δ *srs2*Δ and *rad57*Δ *srs2*Δ (**a**) and *swi5*Δ *srs2*Δ and *sfr1*Δ *srs2*Δ (**c**) backgrounds. Serial dilutions of the indicated cultures were spotted on YES plates containing the given concentrations of drugs. Plates were incubated for the required time (2–4 days) before being photographed. Clonogenic survival of *rrp1*Δ and *rrp2*Δ mutants in *rad57*Δ *srs2*Δ (**b**) and *swi5*Δ *srs2*Δ (**d**) backgrounds. Cells were exposed to 20 μM CPT in liquid culture for the indicated times and plated on YES plates to assess viability. The error bars represent the standard deviation about the mean values. Increase in the level of conversion-type recombinants in *rrp1*Δ and *rrp2*Δ and in *rad57*Δ but not *rad51*Δ mutant background (**e**). Box and whiskers plot, where box represents the range from 25 to 75%, whiskers—the range from 5 to 95%, line dividing the box—the median and a full square—the mean value.

(45,54,55). In this system, *srs2*Δ cells are characterized by an elevated frequency of recombination and an increase in the percentage of conversion-type recombinants, from ~30–50% (54). This is consistent with the proposed role for Srs2 in counteracting Rad51 activity.

We examined the effect of *rrp1*$^+$ and *rrp2*$^+$ deletion, both in wild type and in *rad57*Δ mutant backgrounds, on both the frequency of Ade$^+$ recombinants and proportion of deletion-type and conversion-type outcomes. We observed that the spontaneous HR frequency is not affected in strains devoid of Rrp1 or Rrp2 (result not shown). However, a small but distinct increase in the proportion of conversion-type relative to deletion-type recombinants was observed (Figure 3e). As has been reported for *srs2*Δ (54) the increase in conversion-type Ade$^+$ recombinants was Rad51-dependent, being completely abolished in *rad51*Δ *rrp1*Δ and *rad51*Δ *rrp2*Δ double mutants (Figure 3e). This suggests a role for Rrp1 and Rrp2 in limiting and/or negatively regulating one or more sub-pathways of Rad51-dependent recombination.

Interactions of Rrp1 and Rrp2 with anti-recombinogenic helicase Rqh1

We next examined the genetic interactions of *rrp1*Δ and *rrp2*Δ mutants with *rqh1*Δ. Rqh1 is the *S. pombe* RecQ-like helicase. As observed for *srs2*Δ interactions, the sensitivities of both the *rqh1*Δ *rrp1*Δ and *rqh1*Δ *rrp2*Δ double mutants were not increased when compared with the *rqh1*Δ single mutant (Supplementary Figure S3a and b). We observed a small increase in sensitivity to CPT, MMS and UV of a *rad51*Δ *rqh1*Δ double mutant when compared with the *rad51*Δ single mutant strain, as previously reported for UV (56). Further deletion of *rrp1*$^+$ or *rrp2*$^+$ had no additional effect (Figure 5a, and Supplementary Figure S3c). These data are consistent with Rrp1 and Rrp2 working within a Rad51 pathway. A nonepistatic relationship was apparent for the *rad57*Δ

*rqh1*Δ double mutant on exposure to CPT. Importantly, concomitant deletion of *rrp1*$^+$ or *rrp2*$^+$ in the *rad57*Δ *rqh1*Δ background markedly increased the sensitivity (Figure 5a). In the case of CTP exposure, this approached the level of sensitivity seen in the *rad51*Δ strain. We speculate this relates to the further impairment of the Swi5-dependent SDSA branch of repair (Rrp1 and Rrp2 dependent, see model in Figure 4) in the background incapable of Szostack double HJ repair. This increased CPT sensitivity on deletion of *rrp1*$^+$ or *rrp2*$^+$ is also apparent from survival experiments following acute CPT treatment (Figure 5b). A modest increase in the sensitivity of the triple *rad57*Δ *rqh1*Δ *rrp1*Δ and *rad57*Δ *rqh1*Δ *rrp2*Δ mutants compared with the *rad57*Δ *rqh1*Δ double mutant is also evident on MMS and UV exposure (Supplementary Figure S3c).

We did not observe any nonepistatic interaction between *rqh1*Δ and *swi5*Δ or *sfr1*Δ on CPT exposure. The triple mutants *swi5*Δ *rqh1*Δ *rrp1*Δ and *swi5*Δ *rqh1*Δ *rrp2*Δ also showed the same level of sensitivity as the *rqh1*Δ single mutant (Figure 5c and d). Similar patterns of sensitivity were observed for MMS and UV (Supplementary Figure S3d). These results are consistent with Rrp1 and Rrp2 functioning in parallel to Rqh1 within Swi5/Sfr1 HR sub-pathway, in accordance with the model (Figure 4).

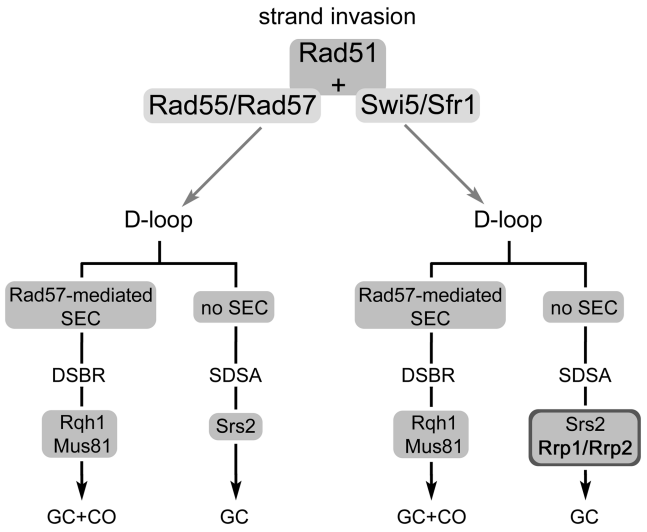

Figure 4. Model of the interactions of Rrp1 and Rrp2 with the mediators of two branches of HR DNA repair pathway and helicases Rqh1 and Srs2. Adapted from (31). See text for details. CO = crossing over, DSBR = double-strand break repair, GC = gene conversion, SEC = second end capture, SDSA = synthesis-dependent strand annealing.

Involvement of Rrp1 and Rrp2 in the response to replication inhibition

When *rqh1*Δ mutant cells are treated with HU, they accumulate unresolved HR intermediates (57,58) leading to aberrant mitosis. This is evidenced by the appearance of cells with cut, fragmented and unequally segregated nuclei (Figure 6a). At a lower frequency, these events also occur in unstressed cells due to endogenous replication problems. Thus, the level of aberrant mitotic events can be used as an indirect readout of unresolved recombination. As has been previously reported (54,57,59), deletion of *rad55*$^+$ or *rad57*$^+$ (and *swi5*$^+$, albeit to a lower level) partially rescues the HU and UV sensitivity of *rqh1*Δ mutants. This has been attributed to the lower incidence of Rad51-dependent recombination events at

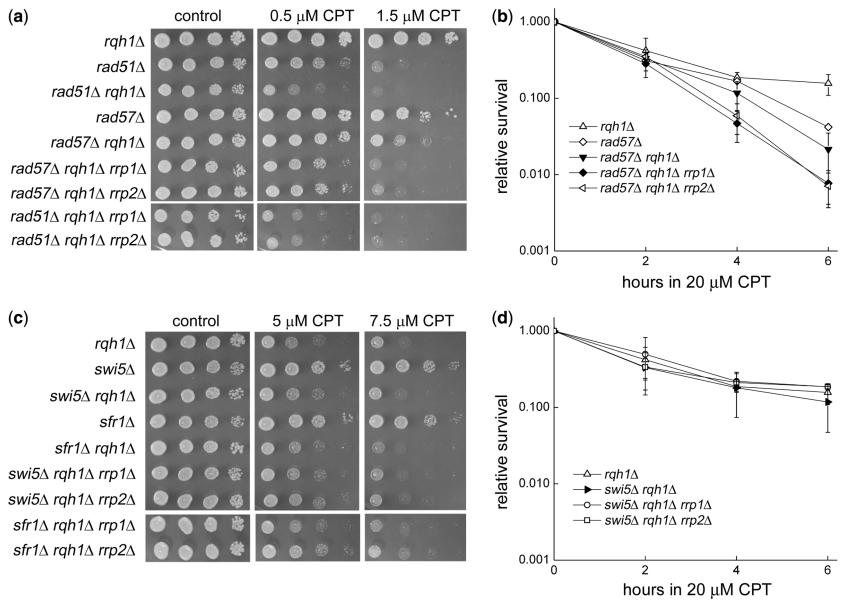

Figure 5. Epistasis between *rrp1*$^+$ and *rrp2*$^+$ and *rqh1*$^+$ helicase gene. Comparison of the sensitivity to CPT of *rrp1*Δ and *rrp2*Δ mutants in *rad51*Δ *rqh1*Δ and *rad57*Δ *rqh1*Δ (**a**) and *swi5*Δ *rqh1*Δ and *sfr1*Δ *rqh1*Δ (**c**) backgrounds. Serial dilutions of the indicated cultures were spotted on YES plates containing the given concentrations of drugs. Plates were incubated for the required time (2–4 days) before being photographed. Clonogenic survival of *rrp1*Δ and *rrp2*Δ mutants in *rad57*Δ *rqh1*Δ (**b**) and *swi5*Δ *rqh1*Δ (**d**) backgrounds. Cells were exposed to 20 μM CPT in liquid culture for the indicated times and plated on YES plates to assess viability. The error bars represent the standard deviation about the mean values.

arrested replication forks: in the absence of HR mediator proteins, recombination is reduced and this alleviates the requirement for Rqh1 in the dissolution of joint molecules.

Deleting *rrp1*$^+$ or *rrp2*$^+$ has no effect on the HU sensitivity *rqh1*Δ or *swi5*Δ *rqh1*Δ (Supplementary Figures S3a and S4a, and Figure 6b). However, deleting either *rrp1*$^+$ or *rrp2*$^+$ in the *rad57*Δ *rqh1*Δ double mutant background partially reversed the rescue of *rqh1*Δ HU sensitivity that occurs due to the deletion of *rad57*$^+$ (Figure 6b and c). Previous genetic data from (57) reported that the triple mutant *rad55*Δ *rqh1*Δ *swi5*Δ was more sensitive to HU when compared with *rad55*Δ *rqh1*Δ. Our data show the same phenomenon for *rad57*Δ *rqh1*Δ *rrp1*Δ and *rad57*Δ *rqh1*Δ *rrp2*Δ, suggesting that Rrp1 and Rrp2 may be involved in the response to replication inhibition. The requirement for Rrp1/Rrp2 proteins for the rescue of the *rqh1*Δ HU sensitivity by *rad57*$^+$ deletion is consistent with their proposed function in a Swi5-dependent SDSA pathway (Figure 4), the only HR sub-pathway available in the *rad57*Δ *rqh1*Δ mutant.

To examine in greater detail the contribution of Rrp1 and Rrp2 following replication inhibition in the *rad57*Δ *rqh1*Δ mutant, we scored the level of aberrant mitotic segregation events in *rad57*Δ *rqh1*Δ *rrp1*Δ and *rad57*Δ *rqh1*Δ *rrp2*Δ and compared these with *rqh1*Δ and *rad57*Δ *rqh1*Δ control cells. We determined the proportion of cells with cut, fragmented and unequally segregated nuclei in cultures treated with 12 mM HU for 4 h and then released into fresh media to recover for a further 4 h. As

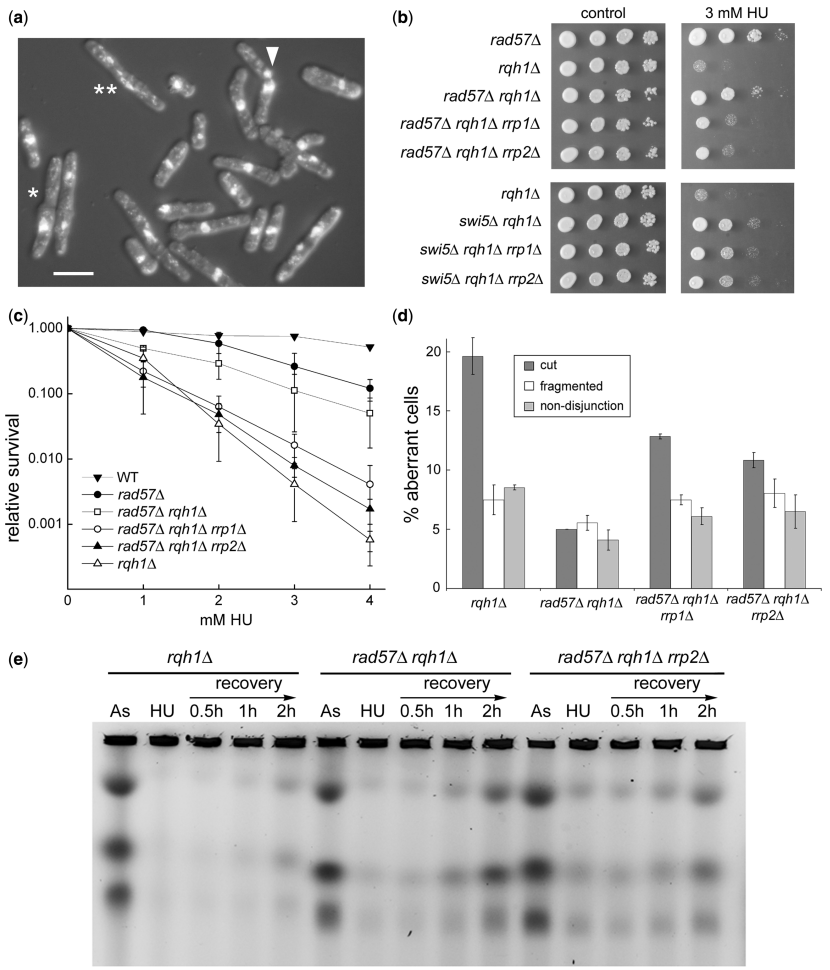

Figure 6. Rescue of *rqh1*Δ mutant HU sensitivity by *rrp1*$^+$ and *rrp2*$^+$ deletion in *rad57*Δ and *swi5*Δ backgrounds. Aberrant cell morphology in *rqh1*Δ mutant after 4 h recovery from 4 h treatment in 12 mM HU (**a**). Cells were fixed in ethanol, stained with DAPI, examined by fluorescence microscopy and photographed. The following aberrant nuclear classes were defined: cut = white down-pointing triangle, nondisjunction = asterisk, fragmented = double asterisk. Scale bar = 10 μm. Comparison of the level of rescue of *rqh1*Δ HU sensitivity conferred by *rrp1*$^+$ or *rrp2*$^+$ deletion in *swi5*Δ (**b**) and *rad57*Δ (b and **c**) backgrounds. Cells were appropriately diluted and spotted or plated on YES plates with different concentrations of HU. Plates were grown for 4–6 days and either photographed or grown colonies counted to determine the relative survival of studied mutants. The error bars represent the standard deviation about the mean values. Quantification of aberrant nuclear phenotypes in mutants with *rrp1*$^+$ or *rrp2*$^+$ deletion in *rad57*Δ *rqh1*Δ background (**d**). Cells were treated for 4 h in 12 mM HU, allowed 4 h to recover, then fixed in ethanol, stained with DAPI and photographed. At least 300 cells were counted for each mutant and assigned to categories defined in (a). PFGE was used to determine the fate of chromosomes following the release from HU treatment (**e**). Replication fork structures and recombination intermediates block the exit of chromosomes from the wells. We compare the behaviour of chromosomes isolated from asynchronous cultures (As), after 4 h treatment in 16 mM HU (HU) and after 0.5, 1 and 2 h from release from replication block (recovery) for *rqh1*Δ, *rad57*Δ *rqh1*Δ and *rad57*Δ *rqh1*Δ *rrp2*Δ mutants.

previously reported for *rad55*Δ *rqh1*Δ (57), the *rad57*Δ *rqh1*Δ double mutant is characterized by substantially lower number of cells with cut or unequally segregated nuclear material when compared with *rqh1*Δ (Figure 6d). This is interpreted as a decrease in the incidence of unresolved replication intermediates in *rad57*Δ *rqh1*Δ when compared with *rqh1*Δ alone. Most probably, this decrease in aberrant mitosis contributes to the increased HU resistance of *rqh1*Δ cells when *rad57*$^+$ is concomitantly deleted. Conversely, the number of cells with cut nuclei and chromosome nondisjunction was markedly increased in the *rad57*Δ *rqh1*Δ *rrp1*Δ and *rad57*Δ *rqh1*Δ *rrp2*Δ triple mutants when compared with the *rad57*Δ *rqh1*Δ double mutant (Figure 6d). This is consistent with increased HU sensitivity observed for both triple mutants described above (Figure 6b and c). We interpret these data to suggest that, in cells lacking both the Rqh1 helicase and the Rad57 mediator protein, Rrp1 and Rrp2 are important for dealing with HR intermediates arising during replication restart in cells recovering from a HU block. The intermediates formed when restarting from HU-arrested replication in *rqh1*Δ *rad57*Δ cells are presumably produced by Rad51 through the Swi5/Sfr1 branch of HR and, if they are not processed by Rrp1/Rrp2, this results in increased missegregation and increased cell death.

If our interpretation is correct, a prediction is that entry of chromosomes into a pulse field gel (PFG) will be delayed in the *rad57*Δ *rqh1*Δ *rrp2*Δ as compared with *rad57*Δ *rqh1*Δ because replication fork structures and recombination intermediates prevent the chromosomes from exiting the wells. First we confirmed that, as previously shown in (57) for *rad55*Δ *rqh1*Δ, chromosomes from a *rad57*Δ *rqh1*Δ mutant reentered a PFG faster than those from the *rqh1*Δ single mutant, consistent with a lower level of entangled chromosomes in the double mutant during recovery from HU treatment. For the triple *rad57*Δ *rqh1*Δ *rrp2*Δ mutant, when compared with *rad57*Δ *rqh1*Δ, chromosomes entered the gel less efficiently during recovery from HU arrest (Figure 6e). This is consistent with the HU sensitivity data and levels of aberrant mitotic events presented above.

Another prediction of our model is that the level of aberrant mitotic segregation events in *swi5*Δ *rqh1*Δ would also be decreased when compared with the *rqh1*Δ single mutant and that further deletion of *rrp1*$^+$ or *rrp2*$^+$ would have no additional effect. Indeed, this is what we observe (Supplementary Figure S4b), which is consistent with Rrp1 and Rrp2 acting in the Swi5/Sfr1 sub-pathway of HR.

Rad51 positively contributes to the response to HU mediated replication inhibition in mutants lacking Rqh1 helicase

Deletion of *rad51*$^+$ has been reported to suppress the HU sensitivity of the *rqh1*Δ mutant (54,59). Indeed, we also observe a slight improvement of growth on HU plates for the *rad51*Δ *rqh1*Δ strain when compared with *rqh1*Δ alone (Figure 7a, and Supplementary Figure S3c). As predicted, concomitant deletion of *rrp1*$^+$ or *rrp2*$^+$ had no effect on this phenomenon. The level of suppression of the HU sensitivity of *rqh1*Δ by *rad51*$^+$ deletion is, however, much less significant than that observed when either *rad57*$^+$ or *swi5*$^+$ are deleted in the *rqh1*Δ background (Figure 7a). Furthermore, the effect gradually disappears with increasing concentrations of HU (Figure 7b). These results are consistent with the reported low level of rescue of the HU sensitivity of *rqh1*Δ cells observed when both *rad55*$^+$ and *swi5*$^+$ are concomitantly deleted (57), as well as with the reduced rescue seen in our *rad57*Δ *rqh1*Δ *rrp1*Δ and *rad57*Δ *rqh1*Δ *rrp2*Δ triple mutants described above. In both cases, Rad51-dependent recombination is seriously impaired.

Interestingly, we observe a dramatically different cell morphology after recovery from HU treatment for mutants in which *rad51*$^+$ is deleted: a significantly lower number of cut cells and of cells showing nondisjunction are present in *rad51*Δ *rqh1*Δ when compared with *rqh1*Δ, despite the fact that cell death is similar in both cases. This decrease is accompanied by the accumulation of very long, often branched, cells and a much higher level of fragmented nuclei (Figure 7c and d). Our interpretation is that, when *rqh1*Δ cells attempt HR, this is toxic and death is accompanied by segregation of chromosomes containing joint molecules. When HR is compromised in these cells (i.e. by loss of Rad51) death occurs, but joint molecules are not made and chromosomes are not physically linked by joint molecules, thus the cut and nondisjunction categories are decreased.

When we consider these data together, they imply that reducing HR—and therefore the production of joint molecules—is the key fact in the rescue of the *rqh1*Δ mutant's HU-induced lethality. However, complete loss of Rad51-mediated recombination is not as effective as reducing its efficacy (Figure 7e). We can conclude from this that Rad51-dependent HR is important for recovering from the replication arrest imposed by HU, both in wild-type cells and in the *rqh1*Δ mutant background. Interestingly, the viability loss in the *rqh1*Δ *rad57*Δ *rrp1*Δ and the *rqh1*Δ *rad57*Δ *rrp2*Δ triple mutants is greater than that seen in the *rqh1*Δ r*ad57*Δ parental strain. We speculate that this is because HR initiated but joint molecules are either more likely to form or are not efficiently resolved. This is consistent with the triple mutants showing a profile of aberrant mitosis more like the *rqh1*Δ mutant alone than the *rqh1*Δ *rad57*Δ double mutant following HU exposure (Figure 6d).

DISCUSSION

We previously reported that Rrp1 and Rrp2 are likely to function in the Sfr1/Swi5-dependent branch of HR repair of DNA DSBs and are also required for replication-coupled repair, as evidenced by the increased sensitivity of *rad57*Δ *rrp1*Δ and *rad57*Δ *rrp2*Δ mutants to agents that induce replication-associated DNA damage including HU, MMS and CPT. Rrp1 and Rrp2 did not function in a redundant manner, so we also suggested they may act together in a complex (42).

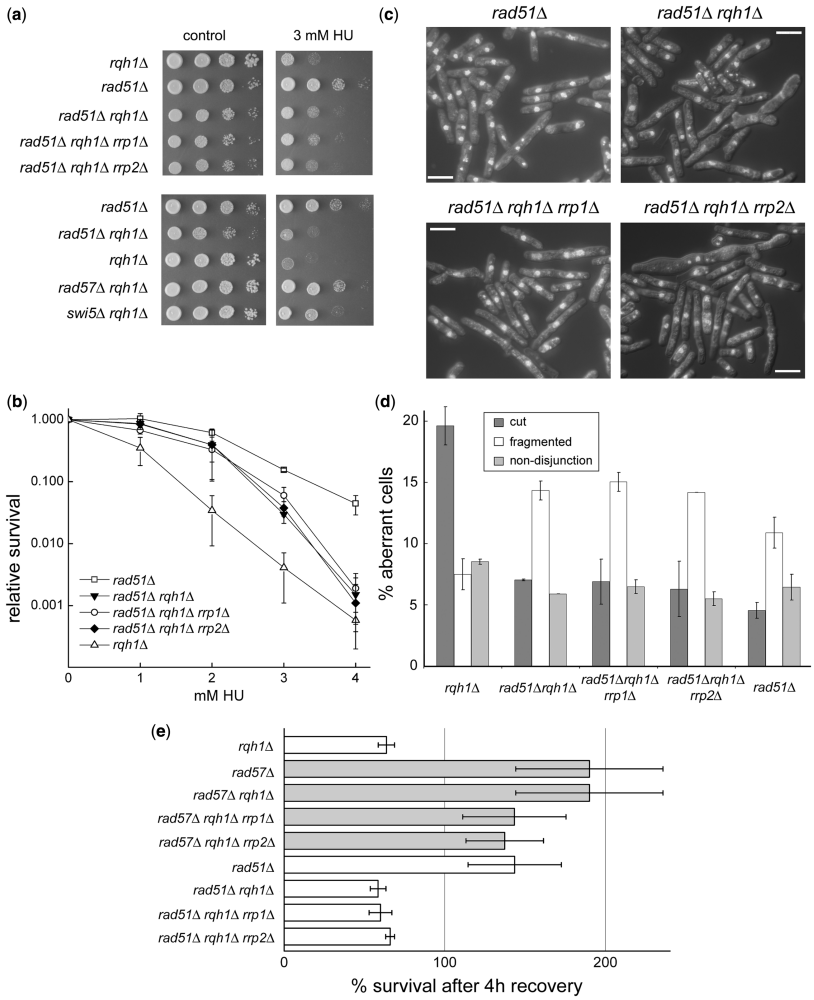

Figure 7. Rescue of *rqh1*Δ mutant HU sensitivity by *rrp1*$^+$ and *rrp2*$^+$ deletion in *rad51*Δ background. Comparison of the level of rescue of *rqh1*Δ HU sensitivity conferred by *rrp1*$^+$ or *rrp2*$^+$ deletion in *rad51*Δ (**a** and **b**) background. Cells were appropriately diluted and spotted or plated on YES plates with different concentrations of HU. Plates were grown for 4–6 days and either photographed or grown colonies counted to determine the relative survival of studied mutants. Aberrant cell morphology in *rad51*Δ, *rad51*Δ *rqh1*Δ, *rad51*Δ *rqh1*Δ *rrp1*Δ and *rad51*Δ *rqh1*Δ *rrp2*Δ mutants after 4 h recovery from 4 h treatment in 12 mM HU (**c**). Cells were fixed in ethanol, stained with DAPI, examined by fluorescence microscopy and photographed. Scale bar = 10 μm. Quantification of aberrant nuclear phenotypes in mutants with *rrp1*$^+$ or *rrp2*$^+$ deletion in *rad51*Δ *rqh1*Δ background (**d**). Cells were treated for 4 h in 12 mM HU, allowed 4 h to recover, then fixed in ethanol, stained with DAPI and photographed. At least 300 cells were counted for each mutant and assigned to categories defined in (Figure 6a). Relative survival of mutants with *rrp1*$^+$ or *rrp2*$^+$ deletion in *rad51*Δ *rqh1*Δ and *rad57*Δ *rqh1*Δ backgrounds (**e**). Cells treated as described above were serially diluted and plated on YES medium to assess viability. The error bars represent the standard deviation about the mean values.

Here, using the yeast 2-hybrid system, we demonstrate that Rrp1 and Rrp2 can interact with each other and also with the Swi5 mediator protein. We also show that Rrp2, like Rrp1 (42), forms MMS-induced foci in the nucleus, which co-localize with Rad52 foci. Because the foci formed by both Rrp1 and Rrp2 also co-localize, we suggest Rrp1 and Rrp2 work together in the HR DNA repair pathway. The formation of Rrp1 and Rrp2 foci in the nucleus following MMS treatment was not dependent on the presence of Rad51, Rad57 or Swi5 proteins, raising the possibility that both Rrp1 and Rrp2 might associate directly with chromatin. Consistent with this, when either gene was cloned into the transcription activating domain containing plasmid, pGADT7, self-activation was observed in two-hybrid system on SD DO-3 plates (Figure 2a). The independence of Rrp1/2 foci formation from Rad51, Rad57 and Swi5 is surprising because other data presented in here suggest a relatively late role for Rrp1 and Rrp2 in the HR. It is possible that Rrp1 and Rrp2 act to help channel recombination into the Swi5/Sfr1-dependent sub-pathway, thus participating in the determination of pathway choice.

Rrp1 and Rrp2 act in concert with Srs2 in HR

To clarify the point of function of Rrp1 and Rrp2 within the Sfr1 HR sub-pathway, we performed epistatic analysis using mutants defective in *rrp1*$^+$ and *rrp2*$^+$ with either *rqh1*Δ or *srs2*Δ in the background of mutants devoid of Rad51, Rad57 or Swi5 functions. We observed a strong synergistic interaction between *srs2*Δ and *rad57*Δ on CPT and MMS and a weaker interaction on HU. These were reminiscent of the phenotypes of the *rad57*Δ *rrp1*Δ and

*rad57*Δ *rrp2*Δ double mutants described earlier (42). The triple mutants *rad57*Δ *srs2*Δ *rrp1*Δ and *rad57*Δ *srs2*Δ *rrp2*Δ exhibited the sensitivity of the double *rad57*Δ *srs2*Δ mutant, raising the possibility that Rrp1 and Rrp2 might function alongside Srs2 in a pathway independent of Rad57. However, we also observed a strong synergistic interaction for *sfr1*Δ *srs2*Δ and *swi5*Δ *srs2*Δ double mutants. The additional deletion of *rrp1*$^+$ or *rrp2*$^+$ in these backgrounds had no further effect, which suggests that Rrp1 and Rrp2, operating with Swi5/Sfr1, function at least partially in an Srs2-independent pathway. To explain our data, we have invoked a model, initially proposed by Akamatsu *et al.* (31), to suggest that Rrp1 and Rrp2 are involved with Srs2 in a Swi5/Sfr1-dependent, but Rad55/Rad57-independent SDSA pathway (Figure 4). This hypothesis was supported when we examined the genetic relationship between Rrp1, Rrp2 and Rqh1: we observed that the CPT and MMS sensitivity of the double *rad57*Δ *rqh1*Δ mutant was higher than that of the respective single mutants and was significantly further increased when either *rrp1*Δ or *rrp2*Δ was introduced. These data are consistent with a role for Rrp1 and Rrp2 in a pathway parallel to both Rqh1 and Rad57, consistent with the model (Figure 4).

Loss of negative regulators of recombination such as the Rqh1 and Srs2 helicases results in elevated recombination frequencies. Additionally, in *srs2*Δ mutants, the proportion of conversion-type recombinants also increases (54). This is consistent with the proposed role for Srs2 in counteracting Rad51 activity. Our examination of recombination outcomes in strains devoid of either the Rrp1 or Rrp2 proteins showed that, while the overall rate of recombination remained unaffected by *rrp1*$^+$ or *rrp2*$^+$ deletion, the proportion of conversion-type recombinants increased in a manner dependent on the presence of the Rad51 recombinase. This suggests that, similar to Srs2, both Rrp1 and Rrp2 function to negatively regulate one or more sub-pathways of Rad51-mediated recombination.

Response of multiple mutants lacking Rqh1 helicase to replication inhibition

We further demonstrated that deletion of *rad57*$^+$, *swi5*$^+$, *sfr1*$^+$ and *rad51*$^+$ in the *rqh1*Δ mutant background leads to a marked decrease in the number of aberrant mitotic events, which are thought to be due to the presence of unresolved HR intermediates. Deletion of each of these genes, with the exception of *rad51*$^+$, also resulted in a pronounced rescue of the HU sensitivity associated with the *rqh1*Δ mutant. Importantly we showed that concomitant deletion of *rrp1*$^+$ or *rrp2*$^+$ reverses this rescue only in the *rad57*Δ *rqh1*Δ mutant. This result, which is reminiscent of the effect observed in (57) for *rad57*Δ *swi5*Δ *rqh1*Δ, strongly supports a function for *rrp1*$^+$ and *rrp2*$^+$ in the Swi5/Sfr1 sub-pathway of HR.

We conclude that abolishing the Rad57-dependent branch of Rad51-mediated HR results in the channeling of the recombination products away from Rqh1-dependent pathways and into the Swi5/Sfr1-, Rrp1/Rrp2- and Srs2-dependent SDSA (the only Rad51-dependent HR sub-pathway remaining in this mutant according to our model, Figure 4). Because, according to the model presented in (31), the absence of Rad55/Rad57 precludes second-end capture, this would be accompanied by the decrease in the number of unresolved joint molecules, allowing Rqh1 depleted cells to recover from HU replication inhibition and leading to the rescue of *rqh1*Δ mutant HU sensitivity. A prediction of this explanation is that compromising the SDSA pathway functioning in *rad57*Δ *rqh1*Δ cells by the concomitant deletion of *rrp1*$^+$ or *rrp2*$^+$ (i.e. the *rad57*Δ *rqh1*Δ *rrp1*Δ and *rad57*Δ *rqh1*Δ *rrp2*Δ triple mutants) would lead to increased cell death following HU treatment because cells would initiate recombination but be unable to resolve SDSA intermediates. Consistent with this prediction, we observe that deletion of *rrp1*$^+$ or *rrp2*$^+$ leads to higher levels of aberrant mitotic events and is detrimental to the triple mutant survival specifically in the *rad57*Δ *rqh1*Δ background (Figure 7e) when compared with the *swi5*Δ *rqh1*Δ background (Supplementary Figure S4c). In the absence of Rad51, cells are unable to initiate HR and chromosomes are not physically linked by joint molecules. Thus, in *rad51*Δ *rqh1*Δ cells, death occurs owing to the problems with restarting replication after HU block, explaining why *rad51*Δ does not rescue *rqh1*Δ HU sensitivity.

A model for the function of Rrp1 and Rrp2

All our results consistently show that Rrp1 and Rrp2 act together with Swi5/Sfr1 but independently of Rad57. Rrp1 and Rrp2 appear to function independently of Rqh1, which is consistent with the proposed requirement for Rad55/Rad57 in Rqh1-dependent canonical Szostack DSBR. Our model places Rrp1 and Rrp2 function in a Swi5/Sfr1-dependent SDSA pathway, together with Srs2. As presented in Figure 4, the model predicts that Swi5/Sfr1-dependent SDSA is the only HR sub-pathway that is independent of Rad57. Our epistasis data thus also corroborate the model proposed by Akamatsu *et al.* (31), which was based on the analysis of recombination products resulting from the repair of an induced DSB.

SUPPLEMENTARY DATA

Supplementary Data are available at NAR Online: Supplementary Table 1, Supplementary Figures 1–4 and Supplementary Reference [60].

ACKNOWLEDGEMENTS

D.D. thanks Ireneusz Litwin for help with cloning *rrp2*$^+$, Sandra Jethon and Natalia Trempolec, former Master students, for initial work on Srs2 helicase. We thank Miguel Ferreira for *rad52-GFP* strain and Felicity Watts for anti-Pmt3 serum. Special thanks to Jo Murray and Matthew C. Whitby for discussions and the kind gift of numerous strains.

FUNDING

Ministry of Science and Higher Education, Poland [N302158737 to D.D.]. A.M.C. acknowledges MRC-UK

Program grant [G1100074]. Funding for open access charge: Statutory funds of Faculty of Biotechnology, Wrocław University.

Conflict of interest statement. None declared.

REFERENCES

1. Symington,L.S. (2002) Role of RAD52 epistasis group genes in homologous recombination and double-strand break repair. *Microbiol. Mol. Biol. Rev.*, **66**, 630–670.
2. Shinohara,A., Ogawa,H., Matsuda,Y., Ushio,N., Ikeo,K. and Ogawa,T. (1993) Cloning of human, mouse and fission yeast recombination genes homologous to RAD51 and recA [erratum in *Nat. Genet.*, 1993 **5**, 312]. *Nat. Genet.*, **4**, 239–243.
3. Krogh,B.O. and Symington,L.S. (2004) Recombination proteins in yeast. *Annu. Rev. Genet.*, **38**, 233–271.
4. Raji,H. and Hartsuiker,E. (2006) Double-strand break repair and homologous recombination in *Schizosaccharomyces pombe*. *Yeast*, **23**, 963–976.
5. Thacker,J. (2005) The RAD51 gene family, genetic instability and cancer. *Cancer Lett.*, **219**, 125–135.
6. Shinohara,A. and Ogawa,T. (1998) Stimulation by Rad52 of yeast Rad51-mediated recombination. *Nature*, **391**, 404–407.
7. New,J.H., Sugiyama,T., Zaitseva,E. and Kowalczykowski,S.C. (1998) Rad52 protein stimulates DNA strand exchange by Rad51 and replication protein A. *Nature*, **391**, 407–410.
8. Osterman,K., Lorentz,A. and Schmidt,H. (1993) The fission yeast *rad22* gene, having a function in mating-type switching and repair of DNA damages, encodes a protein homolog to Rad52 of *Saccharomyces cerevisiae*. *Nucleic Acids Res.*, **21**, 5940–5944.
9. Rijkers,T., Van Den Ouweland,J., Morolli,B., Rolink,A.G., Baarends,W.M., Van Sloun,P.P., Lohman,P.H. and Pastink,A. (1998) Targeted inactivation of mouse RAD52 reduces homologous recombination but not resistance to ionizing radiation. *Mol. Cell. Biol.*, **18**, 6423–6429.
10. Jensen,R.B., Carreira,A. and Kowalczykowski,S.C. (2010) Purified human BRCA2 stimulates RAD51-mediated recombination. *Nature*, **467**, 678–683.
11. Liu,J., Doty,T., Gibson,B. and Heyer,W.D. (2010) Human BRCA2 protein promotes RAD51 filament formation on RPA-covered single-stranded DNA. *Nat. Struct. Mol. Biol.*, **17**, 1260–1262.
12. Feng,Z., Scott,S.P., Bussen,W., Sharma,G.G., Guo,G., Pandita,T.K. and Powell,S.N. (2011) Rad52 inactivation is synthetically lethal with BRCA2 deficiency. *Proc. Natl Acad. Sci. USA*, **108**, 686–691.
13. Liu,J. and Heyer,W.D. (2011) Who's who in human recombination: BRCA2 and RAD52. *Proc. Natl Acad. Sci. USA.*, **108**, 441–442.
14. Sung,P. (1997) Yeast Rad55 and Rad57 proteins form a heterodimer that functions with replication protein A to promote DNA strand exchange by Rad51 recombinase. *Genes Dev.*, **11**, 1111–1121.
15. Khasanov,F.K., Savchenko,G.V., Bashkirova,E.V., Korolev,V.G., Heyer,W.D. and Bashkirov,V.I. (1999) A new recombinational DNA repair gene from *Schizosaccharomyces pombe* with homology to *Escherichia coli* RecA. *Genetics*, **152**, 1557–1572.
16. Tsutsui,Y., Morishita,T., Iwasaki,H., Toh,H. and Shinagawa,H. (2000) A recombination repair gene of *Schizosaccharomyces pombe, rhp57*, is a functional homolog of the *Saccharomyces cerevisiae RAD57* gene and is phylogenetically related to the human *XRCC3* gene. *Genetics*, **154**, 1451–1461.
17. Liu,J., Renault,L., Veaute,X., Fabre,F., Stahlberg,H. and Heyer,W.D. (2011) Rad51 paralogues Rad55-Rad57 balance the antirecombinase Srs2 in Rad51 filament formation. *Nature*, **479**, 245–248.
18. Akamatsu,Y., Dziadkowiec,D., Ikeguchi,M., Shinagawa,H. and Iwasaki,H. (2003) Two different Swi5-containing protein complexes are involved in mating-type switching and recombination repair in fission yeast. *Proc. Natl Acad. Sci. USA*, **100**, 15770–15775.
19. Haruta,N., Kurokawa,Y., Murayama,Y., Akamatsu,Y., Unzai,S., Tsutsui,Y. and Iwasaki,H. (2006) The Swi5-Sfr1 complex stimulates Rhp51/Rad51- and Dmc1-mediated DNA strand exchange *in vitro*. *Nat. Struct. Mol. Biol.*, **13**, 823–830.
20. Jia,S., Yamada,T. and Greval,S.I. (2004) Heterochromatin regulates cell type-specific long-range chromatin interactions essential for directed recombination. *Cell*, **119**, 469–480.
21. Kurokawa,Y., Murayama,Y., Haruta-Takahashi,N., Urabe,I. and Iwasaki,H. (2008) Reconstitution of DNA strand exchange mediated by Rhp51 recombinase and two mediators. *PLoS Biol.*, **6**, e88.
22. Akamatsu,Y. and Jasin,M. (2010) Role for the mammalian Swi5-Sfr1 complex in DNA strand break repair through homologous recombination. *PLoS Genet.*, **6**, e1001160.
23. Yuan,J. and Chen,J. (2011) The role of the human SWI5-MEI5 complex in homologous recombination repair. *J. Biol. Chem.*, **286**, 9888–9893.
24. Tsubouchi,H. and Roeder,G.S. (2004) The budding yeast Mei5 and Sae3 proteins act together with Dmc1 during meiotic recombination. *Genetics*, **168**, 1219–1230.
25. Say,A.F., Ledford,L.L., Sharma,D., Singh,A.K., Leung,W.K., Sehorn,H.A., Tsubouchi,H., Sung,P. and Sehorn,M.G. (2011) The budding yeast Mei5-Sae3 complex interacts with Rad51 and preferentially binds a DNA fork structure. *DNA Rep. (Amst)*, **10**, 586–594.
26. McGlynn,P. and Lloyd,R.G. (2002) Recombinational repair and restart of damaged replication forks. *Nat. Rev. Mol. Cell. Biol.*, **3**, 859–870.
27. Lambert,S., Watson,A., Sheedy,D.M., Martin,B. and Carr,A.M. (2005) Gross chromosomal rearangements and elevated recombination at an inducible site-specific replication fork barrier. *Cell*, **121**, 689–702.
28. Ahn,J.S., Osman,F. and Whitby,M.C. (2005) Replication fork blockage by RTS1 at an ectopic site promotes recombination in fission yeast. *EMBO J.*, **24**, 2011–2023.
29. Lambert,S. and Carr,A.M. (2013) Replication stress and genome rearrangements: lessons from yeast models. *Curr. Opin. Genet. Dev.*, **23**, 132–139.
30. Prudden,J., Evans,J.S., Hussey,S.P., Deans,B., O'Neill,P., Thacker,J. and Humphrey,T. (2003) Pathway utilization in response to a site-specific DNA double-strand break in fission yeast. *EMBO J.*, **22**, 1419–1430.
31. Akamatsu,Y., Tsutsui,Y., Morishita,T., Shahjahan,M.D., Siddique,P., Kurokawa,Y., Ikeguchi,M., Yamao,F., Arcangioli,B. and Iwasaki,H. (2007) Fission yeast Swi5/Sfr1 and Rhp55/Rhp57 differentially regulate Rhp51-dependent recombination outcomes. *EMBO J.*, **26**, 1352–1362.
32. Hope,J.C., Cruzata,L.D., Duvshani,A., Mitsumoto,J., Maftahi,M. and Freyer,G.A. (2007) Mus81-Eme1-dependent and –independent crossovers form in mitotic cells during double strand break repair in *Schizosaccharomyces pombe*. *Mol. Cell. Biol.*, **27**, 3828–3838.
33. Ira,G., Malkova,A., Liberi,G., Foiani,M. and Haber,J.E. (2003) Srs2 and Sgs1-Top3 suppress crossovers during double-strand break repair in yeast. *Cell*, **115**, 401–411.
34. Dupaigne,P., Le Breton,C., Fabre,F., Gangloff,S., Le Cam,E. and Veaute,X. (2008) The Srs2 helicase activity is stimulated by Rad51 filaments on dsDNA: implications for crossover incidence during mitotic recombination. *Mol. Cell.*, **29**, 243–254.
35. Prakash,R., Satory,D., Dray,E., Papusha,A., Scheller,J., Kramer,W., Krejci,L., Klein,H., Haber,J.E., Sung,P. *et al.* (2009) Yeast Mph1 helicase dissociates Rad51-made D-loops: implications for crossover control in mitotic recombination. *Genes Dev.*, **23**, 67–79.
36. Sebesta,M., Burkovics,P., Haracska,L. and Krejci,L. (2011) Reconstitution of DNA repair synthesis in vitro and the role of polymerase and helicase activities. *DNA Rep. (Amst.)*, **10**, 567–576.
37. Sun,W., Nandi,S., Osman,F., Ahn,J.S., Jakovleska,J., Lorenz,A. and Whitby,M.C. (2008) The FANCM ortholog Fml1 promotes recombination at stalled replication forks and limits crossing over during DNA double-strand break repair. *Mol. Cell.*, **321**, 118–128.
38. Mankouri,H.W. and Hickson,I.D. (2007) The RecQ helicase-topoisomerase III-Rmi1 complex: a DNA structure-specific 'dissolvasome'? *Trends Biochem. Sci.*, **32**, 538–546.

39. Morishita,T., Furukawa,F., Sakeguchi,C., Toda,T., Carr,A.M., Iwasaki,H. and Shinagawa,H. (2005) Role of the *Schizosaccharomyces pombe* F-Box DNA helicase in processing recombination intermediates. *Mol. Cell. Biol.*, **25**, 8074–8083.
40. Sun,W., Lorenz,A., Osman,F. and Whitby,M.C. (2011) A failure of meiotic chromosome segregation in a *fbh1*Δ mutant correlates with persistent Rad51-DNA associations. *Nucleic Acids Res.*, **395**, 1718–1731.
41. Lorenz,A., Osman,F., Folkyte,V., Sofueva,S. and Whitby,M.C. (2009) Fbh1 limits Rad51-dependent recombination at blocked replication forks. *Mol. Cell Biol.*, **29**, 4742–4756.
42. Dziadkowiec,D., Petters,E., Dyjankiewicz,A., Karpiński,P., Garcia,V., Watson,A. and Carr,A.M. (2009) The role of novel genes $rrp1^{+}$ and $rrp2^{+}$ in the repair of DNA damage in *Schizosaccharomyces pombe*. *DNA Rep. (Amst.)*, **8**, 627–636.
43. Moreno,S., Klar,A. and Nurse,P. (1991) Molecular genetic analysis of the fission yeast *Schizosaccharomyces pombe*. *Methods Enzymol.*, **194**, 795–823.
44. Craven,R.A., Griffiths,D.J., Sheldrick,K.S., Randall,R.E. and Carr,A.M. (1998) Vectors for the expression of tagged proteins in *Schizosaccharomyces pombe*. *Gene*, **211**, 59–68.
45. Osman,F., Adriance,M. and McCready,S. (2000) The genetic control of spontaneous and UV-induced mitotic intrachromosomal recombination in the fission yeast *Schizosaccharomyces pombe*. *Curr. Genet*, **38**, 113–125.
46. Caspari,T., Dahlen,M., Kanter-Smoler,G., Lindsay,H.D., Hofmann,K., Papadimitriou,K., Sunnerhagen,P. and Carr,A.M. (2000) Characterization of *Schizosaccharomyces pombe* Hus1: a PCNA-related protein that associates with Rad1 and Rad9. *Mol. Cell. Biol.*, **20**, 1254–1262.
47. Cal-Bakowska,M., Litwin,I., Bocer,T., Wysocki,R. and Dziadkowiec,D. (2011) The Swi2–Snf2-like protein Uls1 is involved in replication stress response. *Nucleic Acids Res.*, **39**, 8765–8777.
48. Uzunova,K., Göttsche,K., Miteva,M., Weisshaar,S.R., Glanemann,C., Schnellhardt,M., Niessen,M., Scheel,H., Hofmann,K., Johnson,E.S. *et al.* (2007) Ubiquitin-dependent proteolytic control of SUMO conjugates. *J. Biol. Chem.*, **282**, 34167–34175.
49. Sun,H., Leverson,J.D. and Hunter,T. (2007) Conserved function of RNF4 family proteins in eukaryotes: targeting a ubiquitin ligase to SUMOylated proteins. *EMBO J.*, **26**, 4102–4112.
50. Hecker,C.M., Rabiller,M., Haglund,K., Bayer,P. and Dikic,I. (2006) Specification of SUMO1- and SUMO2-interacting motifs. *J. Biol. Chem.*, **281**, 16117–16127.
51. Mullen,J.R., Chen,C.F. and Brill,S.J. (2010) Wss1 is a SUMO-dependent isopeptidase that interacts genetically with the Slx5-Slx8 SUMO-targeted ubiquitin ligase. *Mol. Cell. Biol.*, **30**, 3737–3748.
52. Gareau,J.R., Reverter,D. and Lima,C.D. (2012) Determinants of small ubiquitin-like modifier 1 (SUMO1) protein specificity, E3 ligase, and SUMO-RanGAP1 binding activities of nucleoporin RanBP2. *J. Biol. Chem.*, **287**, 4740–4751.
53. Mullen,J.R. and Brill,S.J. (2008) Activation of the Slx5-Slx8 ubiquitin ligase by poly-small ubiquitin-like modifier conjugates. *J. Biol. Chem.*, **283**, 19912–19921.
54. Doe,C.L. and Whitby,M.C. (2004) The involvement of Srs2 in post-replication repair and homologous recombination in fission yeast. *Nucleic Acids Res.*, **32**, 1480–1491.
55. Doe,C.L., Osman,F., Dixon,J. and Whitby,M.C. (2004) DNA repair by a Rad22-Mus81-dependent pathway that is independent of Rhp51. *Nucleic Acids Res.*, **32**, 5570–5581.
56. Murray,J.M., Lindsay,H.D., Munday,C.A. and Carr,A.M. (1997) The role of *Schizosaccharomyces pombe* RecQ homolog, recombination and checkpoint genes in UV damage tolerance. *Mol. Cell. Biol.*, **17**, 6868–6875.
57. Hope,J.C., Maftahi,M. and Freyer,G.A. (2005) A postsynaptic role for Rhp55/57 that is responsible for cell death in *rqh1*Δ mutants following replication arrest in *Schizosaccharomyces pombe*. *Genetics*, **170**, 519–531.
58. Win,T.Z., Mankouri,H.W., Hickson,I.D. and Wang,S.W. (2005) A role for the fission yeast Rqh1 helicase in chromosome segregation. *J. Cell Sci.*, **118**, 5777–5784.
59. Miyabe,I., Morishita,T., Hishida,T., Yonei,S. and Shinagawa,H. (2006) Rhp51-dependent recombination intermediates that do not generate checkpoint signal are accumulated in *Schizosaccharomyces pombe rad60* and *smc5/6* mutants after release from replication arrest. *Mol. Cell. Biol.*, **26**, 343–353.
60. Stewart,E., Chapman,C.R., Al-Khodairy,F., Carr,A.M. and Enoch,T. (1997) $rqh1^{+}$, a fission yeast gene related to the Bloom's and Werner's syndrome genes, is required for reversible S phase arrest. *EMBO J.*, **16**, 2682–2692.